A&A 443, 373–381 (2005)
DOI: 10.1051/0004-6361:20053227

Astronomy & Astrophysics

Extended very cold dust in the interacting HI ring galaxy pair NGC 2293 / 2292⋆

M. Stickel[1], D. Barnes[2], and O. Krause[1,3]

[1] Max-Planck-Institut für Astronomie, Königstuhl 17, 69117 Heidelberg, Germany
e-mail: stickel@mpia.de
[2] School of Physics, University of Melbourne, Victoria 3010, Australia
[3] Steward Observatory, University of Arizona, Tucson, AZ 85721, USA

Received 12 April 2005 / Accepted 4 July 2005

ABSTRACT

The LGG 138 galaxy group members NGC 2292 and NGC 2293 were imaged with ISOPHOT in the far-infrared (FIR) at 60 μm, 100 μm, and 200 μm. While no FIR emission is seen at 60 μm, and only very low level emission is present at 100 μm, compact FIR emission from both NGC 2292 and NGC 2293 galaxy centres and extended emission likely associated with tidally removed dust and the HI ring surrounding NGC 2292 / 2293 is strongly detected at 200 μm. Additionally, a compact FIR source associated with the neighbouring galaxy NGC 2295 is strongly detected at 200 μm. Remarkably, none of these three galaxies have been detected individually in 21 cm HI emission. The steeply rising far-infrared spectral energy distribution of the apparently interacting NGC 2292 / 2293 pair towards longer wavelengths indicates the thermal emission of very cold dust with a temperature of 13 K, much lower than typical values of interacting systems or even quiescent spiral galaxies. The FIR data of this galaxy group clearly shows for the first time that there could be FIR dust emission not accompanied by HI, that dust even in an interacting system can have a very low dust temperature, and furthermore that gravitational interaction can give rise to an extended diffuse dust distribution.

Key words. galaxies: individual: NGC 2292 – galaxies: individual: NGC 2293 – galaxies: interactions – intergalactic medium – infrared: general – infrared: galaxies

1. Introduction

Investigation of the atomic hydrogen (HI) emission in a wide variety of galaxies has uncovered, in addition to a smooth distribution, a wealth of different morphologies such as off-centre emission, tails, or ring-like structures. This points in most cases unambiguously to gravitational interactions shaping the distribution of the interstellar medium (ISM) in quite a number of galaxies, even if optical morphologies still appear undisturbed or only weakly disturbed (Hibbard 2000; Hibbard et al. 2001). A particularly rare HI structure is a ring around a single galaxy or a small group of galaxies. Only a handful of such structures are currently recognized (Barnes 1999; Ryan-Weber et al. 2003, and references therein), although more might be hidden among the irregular HI structures collected by Hibbard et al. (2001) and in the HI distributions around S0 galaxies (van Driel & van Woerden 1991).

The HI ring around the NGC 2293 / 2292 galaxy pair is particularly interesting since it is a complete ring (Barnes 1999) in a loose galaxy group (LGG 138, Garcia 1995) rather than only a partial or broken ring structure, such as that surrounding e.g. the M 96 galaxy group (Schneider 1985). Furthermore, the two galaxies inside are not detected as individual HI emitters (Barnes 1999; Rupen et al. 2001). The extended HI had been detected earlier by Huchtmeier et al. (1995) and interpreted as a common halo of the NGC 2293 / 2292 galaxy pair. Additionally, no HI is detected in the nearby distorted dust-lane spiral NGC 2295 (Barnes 1999; Rupen et al. 2001).

The morphological classification of NGC 2292 and NGC 2293 in the literature is somewhat controversial, but both optical brightness profiles clearly follow an exponential disk rather than an elliptical de Vaucouleurs law (Penereiro et al. 1994), which supports the Hubble type S0 rather than E, as given e.g. in NED. The distance to NGC 2293 (the eastern component) derived from surface brightness fluctuations is 17.1 Mpc (Tonry et al. 2001), which will be adopted in the following. It is significantly lower than the distance of ≈27 Mpc derived from the radial velocity and a Hubble constant of $H_0 = 70\,\mathrm{km\,s^{-1}\,Mpc^{-1}}$.

⋆ Based on observations with ISO, an ESA project with instruments funded by ESA Member States (especially the PI countries: France, Germany, the Netherlands, and the United Kingdom) and with the participation of ISAS and NASA.

The apparently interacting galaxy pair NGC 2292 / 2293 (Corwin et al. 1985) shows a break in the $B - R$ color distribution, indicating a younger stellar population inside the HI ring (Barnes 1999). Nevertheless, the two galaxies do not show H α emission lines in their centres (Dahari 1985), and neither is detected in X-rays (O'Sullivan et al. 1999). A CO measurement towards NGC 2293 failed to detect any emission at its systemic velocity of 2025 km s^{-1} (Jorgensen et al. 1995), but remarkably a marginal detection was achieved at ≈2260 km s^{-1} (Huchtmeier & Tamman 1992), very close to the radial velocity of the brightest south-eastern receding side of the HI ring (Barnes 1999). This can be taken as evidence that molecular gas is associated with the ring rather than with NGC 2293 itself, and that possibly also dust could be present there.

Knapp et al. (1989) listed IRAS detections for both NGC 2292 and NGC 2293 at all four IRAS wavelengths. The 60 μm and 100 μm fluxes for the two members of the pair were similar, ≈380 mJy and ≈2800 mJy (as listed in NED), respectively, but the 100 μm fluxes were considered unreliable because of source confusion. Nevertheless, taking the $F_{100\,\mu m}/F_{60\,\mu m}$ flux ratio at face value, this is already a hint for rather low dust temperature in this interacting system. A sub-mm measurement of NGC 2292 by Fich & Hodge (1993) at 450 μm, 800 μm, and 1100 μm found it to be below the detection limits. The aperture used, however, was only 16″ and the chop throw only 60″, which means that for an extended dust distribution the off-position would have been still inside the source, thereby losing much of the source flux. Similarly, the non-detection of NGC 2292 at 10.2 μm by Knapp et al. (1992) used an even smaller aperture and chop-throw of 5.7″ and 30″, respectively, which is again not sensitive to extended emission larger than the chop-throw. These restrictions unfortunately prevent use of these measurements for a combined Near/Mid/Far-infrared spectral energy distribution (SED).

Overall, the limited data available suggest that some kind of interaction has taken place that removed the HI completely from or consumed the HI near the centre of the two galaxies and created the ring, although the sources and interaction partner(s) are not quite clear, as discussed by Barnes (1999). While the molecular gas might have shared the fate of the HI, as indicated by the weak CO detection (Huchtmeier & Tamman 1992), the location of the dust as the third component of the ISM cannot be determined from the IRAS data. Higher sensitivity, higher angular resolution, and an increased wavelength coverage was provided by the ISOPHOT detector aboard the Infrared Space Observatory (ISO; Kessler et al. 1996). Three ISOPHOT FIR maps of the NGC 2293 / 2292 galaxy pair are available in the ISO archive, which allowed a more detailed analysis of the cold dust in this extraordinary system. An additional ISOCAM image at 4.5 μm traces the distribution of the old stellar population. The ISOPHOT observations of NGC 2293 / 2292 are also included in the study of the FIR emission of early type galaxies by Temi et al. (2004), but no detailed analysis of the data has been given.

Barnes (1999) noted the similarity of the HI ring in NGC 2293 / 2292 with the HI ring around IC 2006, an apparently undisturbed E1 galaxy. The distance to IC 2006, as derived from surface brightness fluctuations, is 20.8 Mpc (Tonry et al. 2001), and its radial velocity 1380 km s^{-1}. For IC 2006, the ISO archival data consist of a set of strip maps at four FIR wavelength between 60 μm and 200 μm and a 4.5 μm ISOCAM image, which will be briefly discussed along with the NGC 2293 / 2292 data to show the wide range of FIR properties found in these two apparently similar HI ring systems.

Table 1. Details of ISO observations.

λ [μm]	Detector	Integ. time [s]	Date	ISO TDT
(1)	(2)	(3)	(4)	(5)
NGC 2293 / 2292				
4.5	CAM / LW1	480	Nov. 23, 1997	73801537
60	PHT / C100	990	Oct. 27, 1997	71102227
100	PHT / C100	840	Nov. 24, 1997	73901028
200	PHT / C200	770	Nov. 09, 1997	72401330
IC 2006				
4.5	CAM / LW1	370	Dec. 20, 1997	76501449
60/100	PHT / C100	1960	Jan. 26, 1998	80202007
150/200	PHT / C200	3020	Jan. 23, 1998	79901608

2. Observations and data reduction

An area of ≈15′ × 15′ centred on the NGC 2293 / 2292 galaxy pair has been mapped with chopped raster observations at 60 μm, 100 μm, and 200 μm with the photometer ISOPHOT (Lemke et al. 1996; Lemke & Klaas 1999) aboard the Infrared Space Observatory (ISO). An ISOCAM image at 4.5 μm covers an area of ≈6′ × 3′ along position angle ≈45°. Narrow strip maps across IC 2006 were obtained with ISOPHOT at 60 μm, 100 μm, 150 μm, and 200 μm, and a full map of the inner ≈3′ × 3′ with ISOCAM at 4.5 μm. Details of the observations are listed in Table 1, which gives the wavelength (Col. 1), the detector used (Col. 2), the integration time (Col. 3), the observing date (Col. 4), and the ISO Target Dedicated Time (TDT) number (Col. 5), a unique data set identifier of ISO observations. PI of all observations was G. Knapp, Princeton.

The ISOPHOT data reduction followed the procedures outlined by Stickel et al. (2003), where the signal derivation made use of the distribution of pairwise ramp read-out differences instead of ramp slope fitting, and the final maps were derived from the averaging of a stack of individually drizzled images. The signals were corrected for the dependence on ramp integration times to be consistent with calibration observations, dark-current subtracted, and finally flux calibrated with ISOPHOT Interactive Analysis package PIA[1] Version 9.1/ Cal G Version 6.0 (Gabriel et al. 1997). For the conversion of detector signals to fluxes, the average of the signals of the two FCS measurements accompanying each (sub-)map were used.

[1] The ISOPHOT data presented in this paper were reduced using PIA, which is a joint development by the ESA Astrophysics Division and the ISOPHOT Consortium. The ISOPHOT Consortium is led by the Max-Planck-Institute für Astronomie, Heidelberg.

The ISOCAM data reduction of NGC 2293 / 2292 within IRAF[2] followed standard procedures for ground-based near-infrared (NIR) image stacks, which includes the derivation of a flatfield from the raw image stack, a sliding window background subtraction, and a min-max rejection scheme for the averaging of the drizzled (Hook & Fruchter 1997) individual images. Only the dark level was removed within the ISOCAM Interactive Analysis (Ott et al. 2001) software package, while absolute flux calibration used the standard ISOCAM conversion factor. Because of too small dither shifts, the data reduction for IC 2006 had to make use of a flatfield from a different observation in the same filter. The background was, in this case, modelled by fitting a two-dimensional polynomial of second order to the averaged drizzled stack of individual images and subtracted to give the final map.

The IRAM 30 m telescope was used to search for CO(1−0) and CO(2−1) emission from the south-eastern extension detected in the FIR data, which is positionally coincident with the peak of the HI emission (see below). Both lines were observed simultaneously using SIS heterodyne receivers and the VESPA autocorrelator during a 1.5 h integration on Nov. 6, 2003. The spectra were centred on a redshift of 2260 km s^{-1}, similar to the strongest, south-eastern peak of the HI ring (Barnes 1999), and the weak CO detection of NGC 2293 by Huchtmeier & Tamman (1992). The spectra covered a velocity range of ≈1100 km s^{-1} and ≈500 km s^{-1} for the CO(1−0) and (2−1) lines, respectively. They were smoothed to a resolution of 13 km s^{-1} for analysis, yielding rms noise levels of 8 mK and 13 mK. The beam-width of the CO(1−0) and CO(2−1) observations are 23″ and 11″, respectively.

Since there is considerable disagreement on the radial velocities of the NGC 2293 / 2292 / 2295 galaxy group in the literature, which is reflected in the NED and Simbad database entries for these galaxies, optical spectra were obtained in October 1998 with the RGO spectrograph attached to the 3.9 m Anglo-Australian Telescope. Two 1200 s observations covered the wavelength range between 4500 Å and 6000 Å with a dispersion of 1.6 Å pixel^{-1}, accompanied by CuAr comparison spectra and a spectrum of the star LTT 2415 for flux calibration. Data reduction followed standard procedures within IRAF.

3. Results

3.1. NGC 2293 / 2292 / 2295

The three ISOPHOT FIR maps show a remarkable variation of the FIR morphology of NGC 2293 / 2292 galaxy pair with increasing wavelength. While no emission attributable to the two galaxies is seen at 60 μm (Fig. 1), a weak source centred on the two galaxies is definitely present at 100 μm (Fig. 2). At 200 μm (Fig. 3), the combined two galaxies are strongly detected, with NGC 2293 (eastern component) being the brighter of the pair, which moreover are surrounded by extended emission, most notably towards south-east and north. This towards

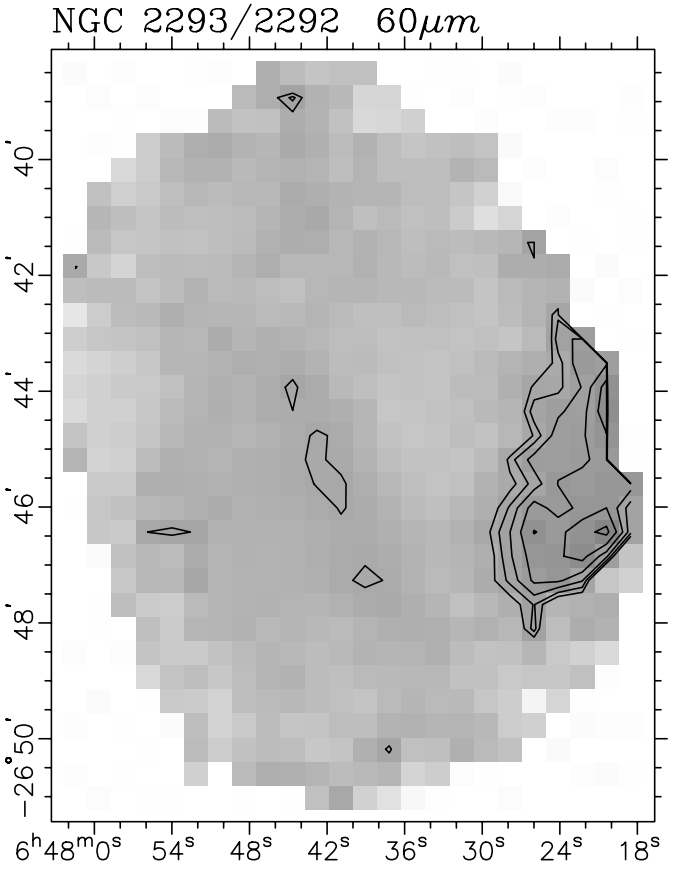

Fig. 1. Gray-scale representation with overlaid isocontours of the background subtracted ISOPHOT 60 μm map of the region centred on NGC 2293/92. Map pixel size is 25″. North is up and east to the left. No FIR emission from the galaxy pair is discernible, while the diffuse feature at the western edge might be attributed to NGC 2295.

longer wavelength steeply rising FIR spectral energy distribution (SED) already indicates that very cold dust is present in this interacting system. The extended area of FIR emission seen in the 200 μm (Fig. 3) map is largely coincident with the extended ring structure seen in the 21 cm HI emission. The very cold and complex extended FIR emission NGC 2293 / 2292 has also been noted by Temi et al. (2004).

Extended FIR emission near the western edge towards NGC 2295 appears to be present in all three maps, but the exact shape cannot be determined from the 60 μm and 100 μm maps due to edge effects, i.e. the redundancy is lower there because not all detector pixels contributed to the final map. However, the somewhat larger 200 μm map (Fig. 3) clearly shows a rather compact bright FIR source surrounded by extended emission, which appears to be associated with the nearby disturbed spiral galaxy NGC 2295.

The optically highly elongated NGC 2295 galaxy is located very close to the edge of the mapped area in each of the three wavelengths, which unfortunately prevents derivation of its SED. Since IRAS did not detect any strong source near NGC 2295 at 100 μm, the 200 μm FIR emission (Fig. 3) also indicates a strongly rising FIR SED and thus very cold dust. From the 200 μm map, a total flux of ≈2 Jy is derived for the integrated FIR emission in the vicinity of NGC 2295.

[2] IRAF is distributed by the National Optical Astronomy Observatories, which are operated by the Association of Universities for Research in Astronomy, Inc., under cooperative agreement with the National Science Foundation.

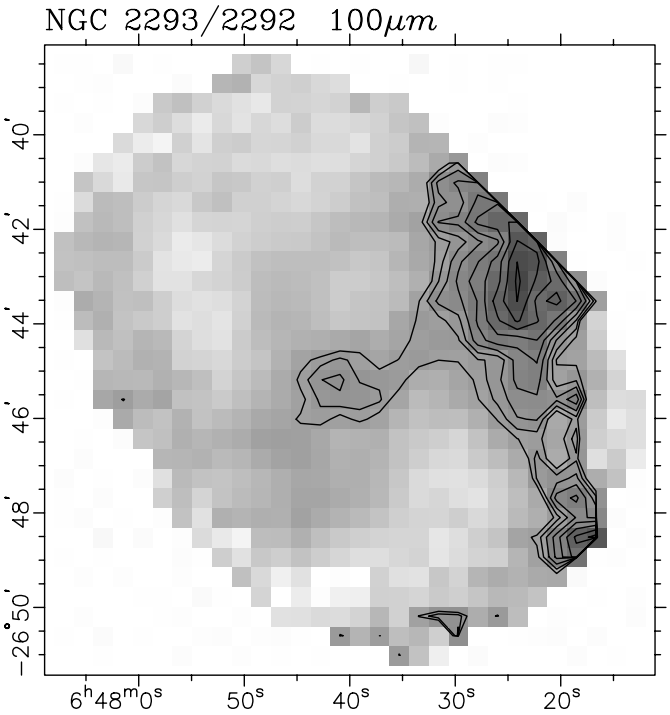

Fig. 2. Gray-scale representation with overlaid isocontours of the background subtracted ISOPHOT 100 μm map. Map pixel size is 25″. North is up and east to the left. Weak FIR emission at the position of NGC 2293/92 is detected in the centre of the map, and extended FIR emission from NGC 2295 is present at the western edge.

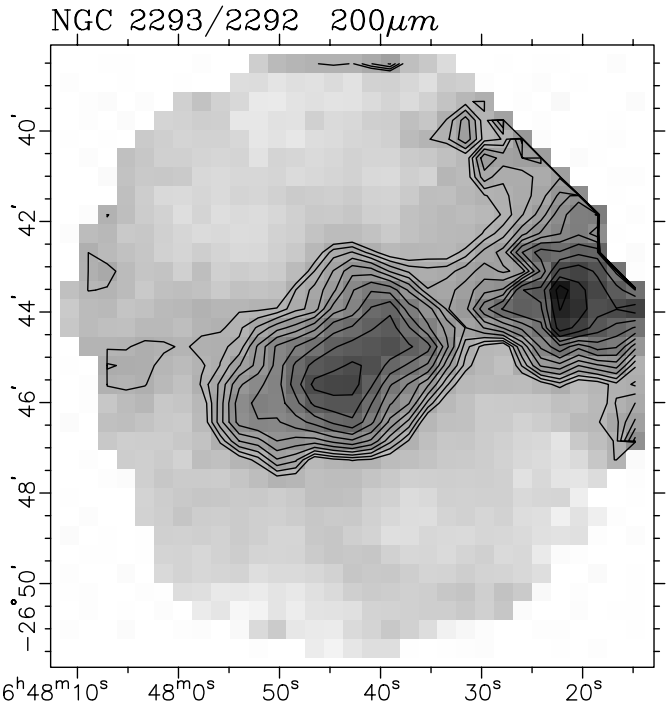

Fig. 3. Gray-scale representation with overlaid isocontours of the background subtracted ISOPHOT 200 μm map. Map pixel size is 25″. North is up and east to the left. Strong FIR emission with extension towards south-east and north is detected at the map centre from the galaxy pair NGC 2293/92, while extended and compact FIR emission near NGC 2295 is present at the western edge.

Due to the small angular distance between NGC 2293 and NGC 2292 of ≈50″ (one pixel of the C100 detector, half a pixel of the C200 detector), the two galaxies are not clearly discernible as separate compact or unresolved FIR sources. Moreover, the diffuse surrounding emission at 200 μm, as well as the only weak detection at 100 μm, prevents a separation of these three different components. Therefore, only the total FIR flux for the combined NGC 2293 / 2292 galaxy pair was measured with simple aperture photometry. The integrated net flux was derived by subtracting various rectangular background boxes from the total flux in a box containing the two galaxies with the surrounding extended emission, while the variations of these differences gave an indication of the accuracy. In the 60 μm map, the flux of the very low level emission near the map centre was taken twice as an upper limit for the 60 μm flux of NGC 2293 / 2292. The resulting fluxes are 720 mJy at 100 μm, 5.30 Jy at 200 μm, while the 60 μm upper limit region is ≈50 mJy. Uncertainties in the 150 μm and 200 μm fluxes are ≈40%, as derived from several combinations of the source and different background regions. The 60 μm upper limit and the flux at 100 μm are a factor ≈5 lower than the IRAS derived values (Knapp et al. 1989).

In the ISOCAM 4.5 μm image (Fig. 4), the two galaxies are clearly resolved, showing a morphology quite similar to the NIR images from the 2MASS Large Galaxy Atlas (Jarrett et al. 2003) and the optical image of Penereiro et al. (1994). Particularly noteworthy is an elongated structure south-east of NGC 2293, which is positionally coincident with an arm- or tidal tail- like feature already seen in the *B*-band DSS-1/2 image. The integrated 4.5 μm flux of both galaxies is ≈80 mJy.

The comparison of the 200 μm map with the optical $B - R$ color image from Barnes (1999) reveals (Fig. 5) that the strongest dust emission is located close to the galaxy centres in a region which coincides with the bluer stellar population there (Barnes 1999). The extended dust emission towards south-east is associated with an optically much redder structure, which lies at the base of the arm or tidal tail extending from there towards south-west, as seen in the DSS-1/2 *B*-band images. It is positionally coincident with the elongated feature south-east of NGC 2293 / 2292 seen in the 4.5 μm image (Fig. 4). A close-up of the $B - R$ color image of this region reveals small radially elongated knots which are even redder than the surrounding medium. The FIR extension towards north also lies at the base of an albeit much fainter arm-like structure seen in the DSS-1/2 *B*-band images, but a detector defect leading to a few dead CCD rows does not allow checking whether there is also a similarly red region there.

The $B - R$ / 200 μm overlay also shows that there is cold dust emission in the region surrounding the nearby disturbed spiral galaxy NGC 2295. Although the peak of the compact FIR source (Fig. 3) is not centred exactly on the optical galaxy, this is most likely due to the coarse sampling with the ISOPHOT C 200 pixels near the map edge. There appears to be some FIR emission of dust lying towards north outside of the disturbed disk of NGC 2295, where the $B - R$ image shows a compact red structure. Overall, the FIR dust emission

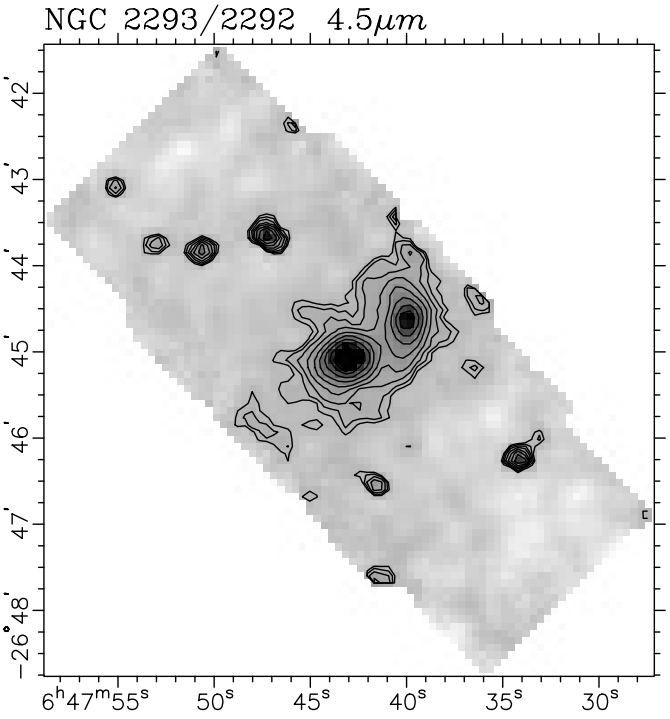

Fig. 4. Gray-scale representation with overlaid isocontours of the background subtracted ISOCAM 4.5 μm map of the region centred on NGC 2293/92. Map pixel size is 5″. North is up and east to the left. NGC 2293/92 is resolved with extended emission surrounding the compact nuclear regions. A detached arm-like feature lies ≈100″ south-east of NGC 2293. Most of the unresolved sources in the field are galactic foreground stars.

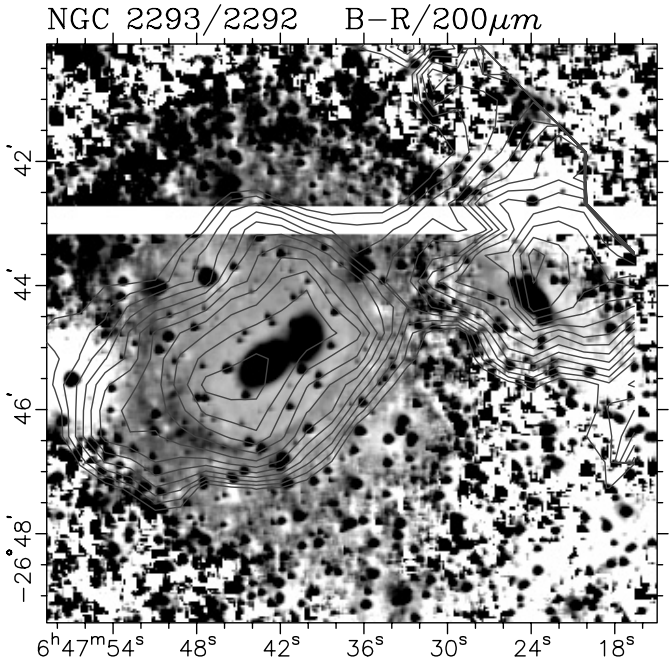

Fig. 5. Gray-scale representation of the optical $B-R$ color image from Barnes (1999) with overlaid isocontours of the ISOPHOT 200 μm map. Coordinates are B1950. Bluer appears lighter, and redder is darker. The bluer region surrounding the two red galaxies cores can be seen clearly. The peak of the cold dust emission is centred on the galaxy pair. The extended dust emission towards south-east coincides with a significantly redder optical feature.

from NGC 2295 and its vicinity appears complex with diffuse dust emission possibly present outside of the main body of the galaxy. This could be due to the gravitational interaction, which also disturbed the disk.

The column density of the HI ring has its maximum at the position of the optically red structure described above, which in turn is coincident with the extended FIR emission south-east of NGC 2293 / 2292 (Fig. 6). Overall, dust emission is seen throughout the HI ring area, but appears to be generally shifted slightly towards south. The maximum of the FIR emission is not exactly coincident with the hole of the HI column density, although this might also be an artifact due to the coarse sampling of the FIR emission with the large (1.5′) C200 detector pixels.

The steep flux increase of the integrated FIR SED towards longer wavelengths (Fig. 7) with a $F_{200\,\mu\mathrm{m}}$ / $F_{100\,\mu\mathrm{m}}$ flux ratio of ≈7 is indicative of the thermal emission from a very cold dust component with a temperature far below $T_{\mathrm{Dust}} \approx 17$ K, the average value of the Milky Way (Sodroski et al. 1994) and other normal inactive spiral galaxies (Stickel et al. 2000). The dust emission is usually characterized by a modified blackbody (Planck) function

$$F_\nu \propto \nu^\beta \, B_\nu \, (T_{\mathrm{Dust}}) \tag{1}$$

with a dust color temperature T_{Dust} and an emissivity index β. For the Milky Way, an inverse temperature dependence of the emissivity index is found (Dupac et al. 2003). If this relation also holds for the dust in NGC 2293 / 2292, then only $\beta \approx 2$ is appropriate for deriving a dust color temperature. The detections at 100 μm and 200 μm, together with the upper limit at 60 μm, can then be reconciled with a dust color temperature $T_{\mathrm{Dust}} \approx 13$ K (with $\beta = 2$). The FIR spectrum (Fig. 7) shows that the peak of the FIR emission likely lies near 200 μm.

Given the FIR flux F_ν at 200 μm, the dust color temperature T_{Dust} and distance D, the dust mass associated with the FIR emission can be derived from

$$M_{\mathrm{Dust}} = D^2 \, F_\nu \, [\kappa_\lambda \, B_\nu(T_{\mathrm{Dust}}) \,]^{-1} \tag{2}$$

(Hildebrand 1983; Draine 1990), where the dust opacity κ_λ encompasses all grain properties such as the size distribution, density, and composition. Dust opacities are rather uncertain and a representative value of 3 m^2/kg for 200 μm is used, which lies in the middle of the range of currently considered values (Draine 1990). Using the distance of 17.1 Mpc to NGC 2293 (Tonry et al. 2001) as representative of the whole extended FIR emission, the derived dust mass for a dust color temperature $T_{\mathrm{Dust}} = 13$ K is $M_{\mathrm{Dust}} \approx 1.2 \times 10^7 \, M_\odot$. Taking the redshift-based distance of 27 Mpc (using a Hubble constant of $H_0 = 70$ km s^{-1} Mpc^{-1}), the dust mass would be higher by a factor of ≈2.5. This combined derived dust mass for the two galaxies is neither extremely low nor exceptionally high, but instead is representative of the majority of inactive spiral galaxies found e.g. in the ISOPHOT Serendipity Survey (Stickel et al. 2000).

The weak detection of CO (1–0) at the position of NGC 2293 with roughly the radial velocity of the receding

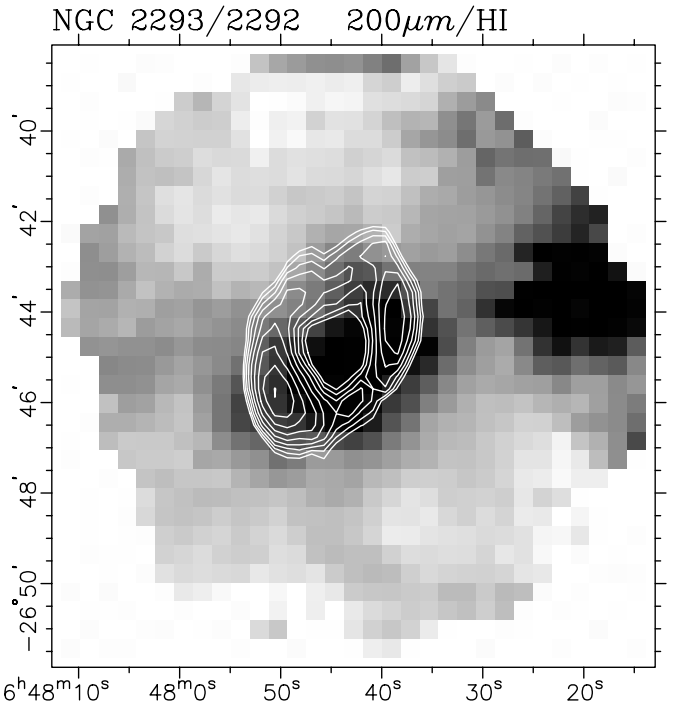

Fig. 6. Gray-scale representation of the ISOPHOT 200 μm map with overlaid isocontours of the HI column density (Barnes 1999). The dust emission peaks near but slightly south of the hole of the HI ring structure. The extended dust emission towards south-east (cf. 3) coincides with the strongest HI emission.

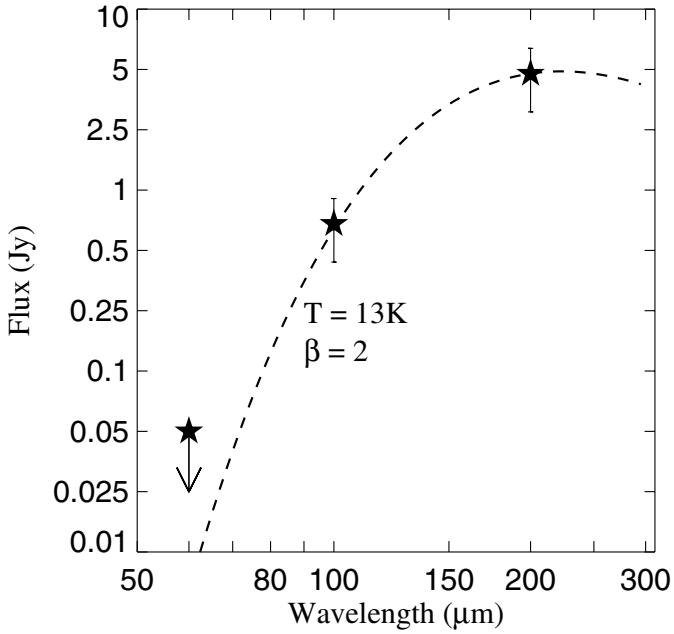

Fig. 7. Integrated FIR spectrum of the NGC 2293/92 galaxy pair. The dashed curve shows a modified blackbody spectrum with temperature $T_{\rm Dust}$ = 13 K and emissivity $\beta = 2$. 40% error bars are indicated for the ISOPHOT detections at 100 μm and 200 μm.

south-eastern side of the HI ring (Huchtmeier & Tamman 1992) indicated that even the molecular gas is in an unusual dynamical stage. Unfortunately, the newly acquired CO spectrum at the position of the south-eastern extended FIR emission ≈15 kpc away from NGC 2293 failed to detect any significant emission in either line, although a very weak broad emission feature might be present in the CO (2–1) spectrum at the expected velocity. Clearly, these non-detections should definitely be improved with a much longer integration time, to check whether NGC 2293 might be a further member of the rare group of galaxies with off-center molecular gas (Braine et al. 2001; Aalto et al. 2001).

The optical spectra did not show any emission lines of either Hβ λ4861 or [OIII] $\lambda\lambda$5945, 5007, corroborating the result of Dahari (1985), even though the galaxies in this group are apparently interacting. The redshift was therefore derived from stellar absorption features of FeI λ4529, Hβ λ4861, MgI λ5175, and NaI λ5893. The resulting radial velocities are 2010 km s^{-1}, 2320 km s^{-1}, and 1850 km s^{-1} for NGC 2293 NGC 2292 and NGC 2295, respectively, with uncertainties of 20–40 km s^{-1}, as judged from the velocity variations of the measured absorption features. These values agree with those listed in Barnes & Webster (2001), which were carefully selected from the literature. The values for NGC 2293 and NGC 2292 listed in Simbad, which were taken from Garcia (1993), are too small by more than 200 km s^{-1}, while the redshift for NGC 2292 listed in NED, which was taken from Huchtmeier et al. (1995), also is too small by more than 200 km s^{-1}. The spectral resolution was not high enough to allow the investigation of the front-to-back ordering of NGC 2293 relative to NGC 2292 by searching for absorption features of one galaxy in the spectrum of the other, an issue of great importance for the dynamical stage of the group (Barnes 1999). If anything, the absorption features of NGC 2293 were found to be slightly broader than those of NGC 2292, which might be an indication of an overlap between two absorption systems in the sense that the higher redshift system of NGC 2292 is in front of the lower redshift system of NGC 2293. However, an unequivocal clarification would require higher spectral resolution data with much longer integration time.

3.2. IC 2006

Although the HI ring morphology of IC 2006 appears to be similar to that of NGC 2293 / 2292 (Barnes 1999), comparison of the ISOPHOT images of NGC 2293 / 2292 and IC 2006 strikingly shows a large difference in the FIR properties. Three of the four maps between 60 μm and 200 μm show no reliable trace of emission from either the galaxy centre or the surrounding HI ring structure (Fig. 8). From the variations across the maps, upper limits of ≈60 mJy can be derived, unless the FIR emission is diffuse and extended over a large fraction of the available maps. Only at 100 μm, a weak compact source centred at the position of the galaxy appears to be detected. Its flux is ≈100 mJy. Given the weakness of the FIR emission from IC 2006, these limits and the detection at 100 μm are consistent with the IRAS values given by Knapp et al. (1989). As expected, the 4.5 μm ISOCAM image (Fig. 9) shows the resolved appearance from the star light of the elliptical galaxy with a total flux of ≈50 mJy, but possibly also a central unresolved core.

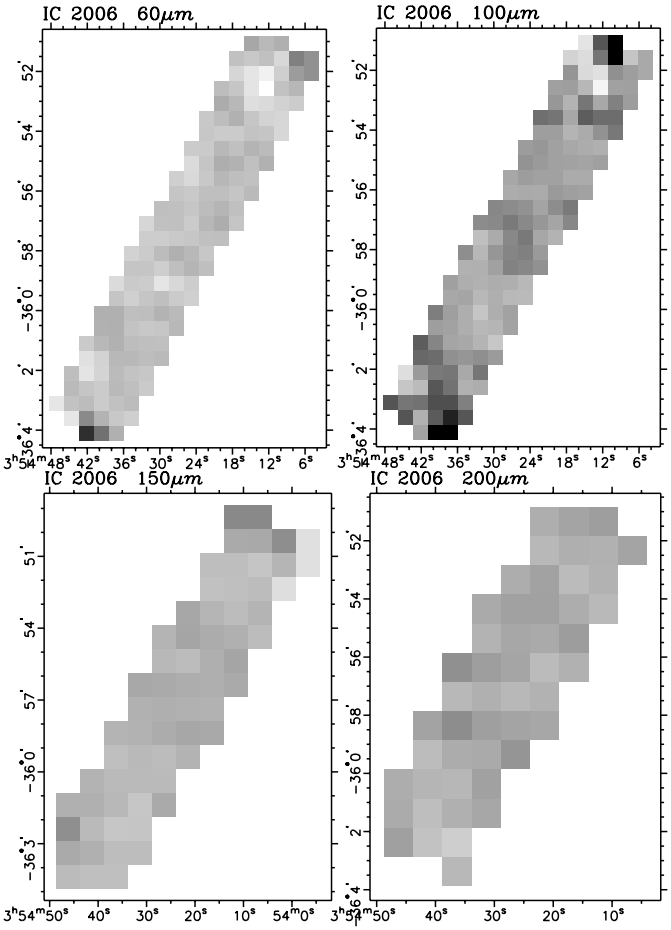

Fig. 8. Gray-scale representation of the ISOPHOT 60 μm (*upper left*), 100 μm (*upper right*), 150 μm (*lower left*), and 200 μm (*lower right*) strip maps centred on IC 2006. North is up and east to the left. Map pixel size is 25″, and 50″ for the upper and lower two maps, respectively. Only at 100 μm, a weak detection ($F_{100\,\mu\mathrm{m}} \approx 100$ mJy) is present, while the three other wavelengths only give upper limits of ≈60 mJy.

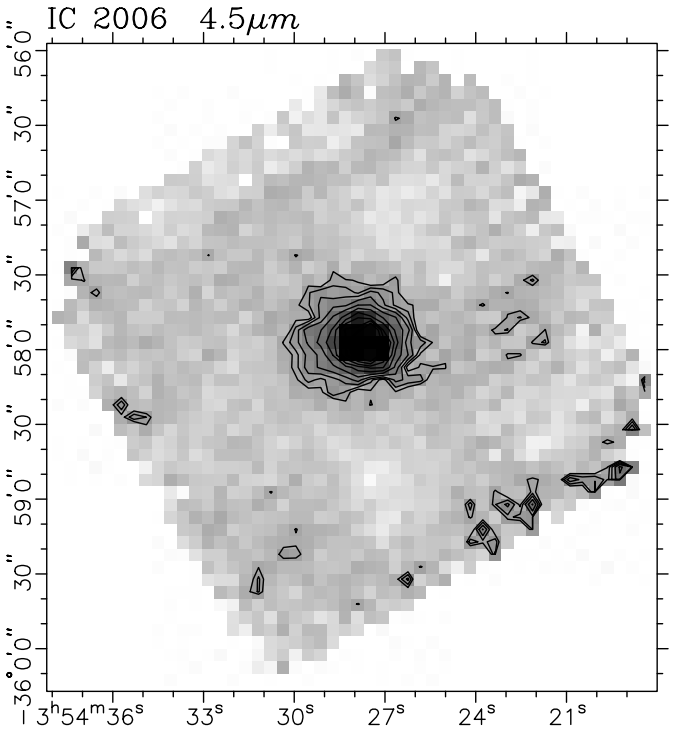

Fig. 9. Gray-scale representation with overlaid isocontours of the ISOCAM 4.5 μm map of the region centred on IC 2006. Map pixel size is 5″. North is up and east to the left. Extended emission surrounding a possibly unresolved core is present.

Overall, its appearance is quite similar to that of the S0 galaxy NGC 3998 (Knapp et al. 1996). Unfortunately, the image is too small to allow detection of the HI ring of IC 2006 with its 2′ radius (Schweitzer et al. 1989).

The detection at 100 μm and non-detections at the other wavelengths might be taken as evidence that the SED of the dust emission actually peaks around 100 μm, which means that the dust in IC 2006 would be rather warm, with dust temperatures lying in the range 25 K−30 K. Using the 100 μm flux, a dust opacity of 6 m^2/kg, and other parameters as above, the associated dust mass lies in the range $1 \times 10^4\,M_\odot \lesssim M_{\mathrm{Dust}} \lesssim 3 \times 10^4\,M_\odot$, much lower than the dust mass in NGC 2293 / 2292, and also about a factor 10 lower than that of the elliptical/S0 galaxy sample studied by Bregman et al. (1998).

4. Discussion

The NGC 2293 / 2292 galaxy pair has several unusual properties, which sets it apart from other galaxy groups, particularly with interacting members, which have hitherto been studied in the FIR. Most outstanding is the extremely high 170/100 integral flux ratio of ≈7, one of the highest ratios of all single galaxies or pairs measured in the FIR range so far, close to the coldest galaxies found in the ISO observations of the Virgo Cluster galaxy sample (Popescu et al. 2002; Tuffs et al. 2002). Its immediate implication is the very cold dust color temperature of only 13 K, much lower than the average value of the Milky Way (Sodroski et al. 1994) and other normal inactive spiral galaxies (Stickel et al. 2000). Deriving similar low dust temperatures in other interacting galaxies has as yet been possible only with the use of sub-mm data (e.g., Haas et al. 2000).

This very low dust temperature is even more unusual, since the NGC 2293 / 2292 2295 group is an apparently interacting system, for which much higher dust color temperatures, mostly from IRAS 60 μm and 100 μm data, have usually been inferred (e.g., Horellou & Booth 1997; Bushouse et al. 1998, and references therein). This is also the first detection of cold dust with such a very low temperature in a galaxy group based on FIR data alone. Only the 200 μm data clearly reveal the presence of the dust in these galaxies, while the shorter wavelengths 100 μm only give a weak detection (Figs. 2 and 3).

As a consequence, galaxies or galaxy groups with similar low dust temperatures and low 100 μm FIR fluxes of $\lesssim$1 Jy have most likely up to now escaped detection because the IRAS survey only hardly reached this detection limit, while in shorter wavelengths data such objects are not present and longer wavelengths data are still scarce. Moreover, given the large discrepancy of a factor 5 between the uncertain IRAS flux and the

ISOPHOT 100 μm flux, similar cases may just not have been recognized because of the overestimation of the IRAS fluxes and the resulting too-high derived dust color temperatures. A first step towards finding more such very cold galaxies might be the galaxy catalogue from the ISOPHOT Serendipity Survey (Stickel et al. 2004b), where a number of 170 μm detections had no counterparts at the shorter IRAS wavelengths. Clearly, follow-up observations are required to secure the FIR emission and the implied low dust temperatures of these sources.

This is also the first unambiguous detection of extended FIR emission outside galaxies due to cold dust in an interacting galaxy group, thereby strengthening the concept of dust removal via gravitational interaction (Stickel 2004). The detection of FIR emission from an optically visible dust structure ≈15 kpc south-east of NGC 2293 at the base of a tidal arm, as well the diffuse FIR emission surrounding NGC 2295, shows that gravitational interactions can spread dust across large regions from the galaxy centres and move dust structures out of the disks.

A break in the $B - R$ color of NGC 2293 / 2292 distribution has been observed (Barnes 1999), where the region inside the HI ring closer to the two galaxy centres is bluer by 0.2 mag than outside (see also Fig. 5). This indicates a younger stellar population, but nevertheless the dust there has apparently not being heated by the strong UV radiation of recently formed stars. This is also supported by the absence of detectable 60 μm emission, which is usually at least partially attributed to a warmer dust component from very small grains. Gravitational interactions therefore are not necessarily accompanied by vigorous star formation, which in turn will significantly heat the dust. This accords with several studies of interacting galaxies, which also did not find a significantly enhanced FIR emission or increased dust temperatures (Bergvall et al. 2003, and references therein). In fact, in the case of the NGC 2293 / 2292 galaxy pair, a process capable of reducing the dust temperature below that found in normal inactive galaxies, which are still star-forming at a low level, seems to be necessary.

HI is detected only in a ring, where the maximum is closely coincident in position with extended dust emission towards the south-east. The total HI mass rescaled to a distance of 17.1 Mpc is $M_{\rm HI} \approx 0.75 \times 10^9\, M_\odot$ (Barnes 1999), while the upper limit to the (rescaled) mass of molecular hydrogen is $M_{\rm H_2} \lesssim 7 \times 10^7\, M_\odot$ (Huchtmeier & Tamman 1992), which together with the dust mass of $M_{\rm Dust} \approx 1.2 \times 10^7\, M_\odot$ gives a gas-to-dust ratio of only ≈60, much lower than that of the Milky Way and at the lower end of the distribution of normal inactive spiral galaxies (Stickel et al. 2000). Since the two galaxies are not detected individually in HI while strong FIR emission from cold dust is clearly detected, the inferred gas-to-dust ratio for the inner region of the NGC 2293 / 2292 pair is much smaller. Assuming that ≈75% of the dust mass is near the galaxy centres, and the upper limit for the HI gas in both galaxies is $M_{\rm HI} < 10^7\, M_\odot$ (Barnes 1999, converted to 17.1 Mpc), then the upper limit for the gas-to-dust ratio in the inner regions of the galaxies is ≲1. The situation is similar for NGC 2295 since there is cold dust emission in the area close to and surrounding the galaxy, although no HI has been detected (Barnes 1999; Rupen et al. 2001). Either the gas has been separated from the dust in all three galaxies by a dynamical process, or has been converted to stars without the usual consequence of strong dust heating by a young stellar population. Conversely, the low overall gas-to-dust ratio might be taken as evidence that the large spread seen in the gas-to-dust ratio of normal inactive spiral galaxies (Stickel et al. 2000) might at least be partially caused by gravitational encounters and the resulting consumption by star formation or tidal removal of neutral HI gas. This raises some doubts about the common practice of using a standard gas-to-dust ratio for deriving gas masses from FIR luminosities across a broad variety of galaxy types.

Overall, the distortions seen in the NGC 2293 / 2292 / 2295 triplet bear some resemblance to Stephan's Quintet (Arp 319), an interacting galaxy group with optically disturbed members (Gutierrez et al. 2002), where most of the HI is located outside of the galaxies (Williams et al. 2002). Large radial velocity differences of several 100 km s^{-1} are also seen there, similar to that found in NGC 2293 / 2292 / 2295. Extended FIR emission is also present throughout the group (Xu et al. 2003; Stickel 2004), but the temperature of the diffuse dust there is most likely higher since it is already detected at 100 μm. The NGC 2293 / 2292 / 2295 group might thus either be less violently interacting or is in a different earlier or later stage, where star formation has not yet been started or has already died out, which also can explain the missing emission lines in the galaxy centres (Dahari 1985). If large scale very cold dust distributed outside galaxies is common in such interacting groups, it will go undetected as FIR measurements near 200 μm are necessary and only few groups have been imaged with ISOPHOT at these long FIR wavelengths. Particularly missing is an FIR map of Stephan's Quintet at an FIR wavelength beyond 100 μm to study the distribution of the cold dust in this group. A further example of cold dust spread across an interacting galaxy group may be CG 1720-67.8 (Weinberger et al. 1999), where optical spectra revealed a strong optical extinction and significant star-forming activity, yet the group is not detected in the IRAS bands.

The detected cold dust in the HI ring structure around NGC 2293 / 2292 clearly shows that at least this HI ring is most likely not primordial (Knapp 1999). The HI ring around IC 2006, which is not detected in the FIR, however, could in fact be a remnant from the early collapse of the central elliptical, although a tidal capture of either an unevolved HI-rich and metal-poor dwarf or of the outer halo regions of a low surface brightness galaxy also is a viable alternative. Clearly, the apparently similar HI rings around NGC 2293 / 2292 and IC 2006 can have quite different origins.

Assuming that the origin of the HI rings is a gravitational interaction in both NGC 2293 / 2292 and IC 2006, FIR observations can hint at the type of the progenitor galaxies. If apparently similar HI features have a similar history, the detected gas can nevertheless have its origin in different types of progenitor galaxies. In the case of NGC 2293 / 2292, it very likely has been gas and dust rich, while in the case of IC 2006 it is likely to have been gas rich but dust poor. The prospect of FIR measurements is then to break the degeneracy of other indicators and to provide independent clues to the history of such events (Stickel et al. 2004a).

The currently rather limited data on NGC 2293 / 2292 / 2295 presented here clearly indicate that this is a highly unusual gravitationally interacting group. Nevertheless, a more detailed understanding of this system definitely requires new high resolution FIR, HI, and CO data, which would allow a separate investigation of the galaxy centres, the surrounding bluer region, and the dust structures seen towards south-east across a large wavelengths range. Obviously equally interesting are the compact and diffuse FIR emission near NGC 2295, which is only partially covered by the ISOPHOT data.

Acknowledgements. We thank Rachel Webster for initiating the spectroscopic observations of NGC 2292 / 2293 / 2295. The development and operation of ISOPHOT were supported by MPIA and funds from Deutsches Zentrum für Luft- und Raumfahrt (DLR, formerly DARA). The ISOPHOT Data Centre at MPIA is supported by Deutsches Zentrum für Luft- und Raumfahrt (DLR) with funds of Bundesministerium für Bildung und Forschung, grant. No. 50 QI0201. This research made use of NASA's Astrophysics Data System Abstract Service, the Simbad Database, operated at the CDS, Strasbourg, France, and data from the Infrared Processing and Analysis Center (IPAC) and the NASA/IPAC Extragalactic Database (NED), which are operated by the Jet Propulsion Laboratory, California Institute of Technology, under contract with the National Aeronautics and Space Administration. It is based on photographic data obtained using The UK Schmidt Telescope operated by the Royal Observatory Edinburgh, with funding from the UK Science and Engineering Research Council, until 1988 June, and thereafter by the Anglo-Australian Observatory. Original plate material is copyright © the Royal Observatory Edinburgh and the Anglo-Australian Observatory. The plates were processed into the present compressed digital form with their permission. The Digitized Sky Survey was produced at the Space Telescope Science Institute under US Government grant NAG W-2166.

References

Aalto, S., Hüttemeister, S., & Polatidis, A. G. 2001, A&A, 372, L29
Barnes, D. G. 1999, PASA, 16, 77
Barnes, D. G., & Webster, R. L. 2001, MNRAS, 324, 859
Bergvall, N., Laurikainen, E., & Aalto, S. 2003, A&A, 405, 31
Braine, J., Duc, P.-A., Lisenfeld, U., et al. 2001, A&A, 378, 51
Bregman, J. N., Snider, B. A., Grego, L., & Cox, C. V. 1998, ApJ, 499, 670
Bushouse, H. A., Telesco, C. M., & Werner, M. W. 1998, AJ, 115, 938
Corwin, H. G., de Vaucouleurs, A., & de Vaucouleurs, G. 1985, Southern Galaxy Catalogue, Univ. Texas Monographs in Astronomy
Dahari, O. 1985, ApJS, 57, 643
Draine, B. T. 1990, in The Interstellar Medium in Galaxies, ed. H. A. Thronson Jr., & J. M. Schull (Dordrecht: Kluwer), 483
van Driel, W., & van Woerden, H. 1991, A&A, 243, 71
Dupac, X., Bernard, J.-P., Boudet, et al. 2003, A&A, 404, L11
Fich, M., & Hodge, P. 1993, ApJ, 415, 75
Gabriel, C., Acosta-Pulido, J., Heinrichsen, I., et al. 1997, Astronomical Data Analysis Software and Systems VI, ed. G. Hunt, & H. E. Payne, ASP Conf. Ser., 125, 108
Garcia, A. M. 1993, A&AS, 100, 47
Garcia, A. M. 1995, A&A, 297, 56
Gutierrez, C. M., Lopez-Corredoira, M., Prada, F., & Eliche, M. C. 2002, ApJ, 579, 592
Haas, M., Klaas, U., Coulson, I., Thommes, E., & Xu, C. 2000, A&A, 356, L83
Hibbard, J. E. 2000, in Dynamics of Galaxies: from the Early Universe to the Present, ed. F. Combes et al., ASP Conf. Ser., 197, 285
Hibbard, J. E., van Gorkom, J. H., Rupen, M. P., & Schiminovich, D. 2001, in Gas and Galaxy Evolution, ed. J. E. Hibbard et al., ASP Conf. Ser., 240, 657
Hildebrand, R. H. 1983, QJRAS, 24, 267
Hook, R. N., & Fruchter, A. S. 1997, Astronomical Data Analysis Software and Systems VI, ed. G. Hunt, & H. E. Payne, ASP Conf. Ser., 125, 147
Horellou, C., & Booth, R. 1997, A&A, 126, 3
Huchtmeier, W. K., & Tamman, G. A. 1992, A&A, 257, 455
Huchtmeier, W. K., Sage, L. J., & Henkel, C. 1995, A&A, 300, 675
Jarrett, T. H., Chester, T., Cutri, R., et al. 2003, AJ, 125, 525
Jorgensen, I., Franx, M., & Kjaergaard, P. 1995, MNRAS, 276, 1341
Kessler, M. F., Steinz, J. A., Anderegg, M. E., et al. 1996, A&A, 315, L27
Knapp, G. R., Guhathakurta, P., Kim, D.-W., & Jura, M. 1989, ApJS, 70, 329
Knapp, G. R., Gunn, J. E., & Wynn-Williams, C. G. 1992, ApJ, 399, 76
Knapp, G. R., Rupen, M. P., Fich, M., et al. 1996, A&A, 315, L75
Knapp, G. R. 1999, in Star Formation in Early Type Galaxies, ed. P. Carral, & J. Cepa, ASP Conf. Ser., 163, 119
Lemke, D., Abolins, J., Abraham, P., et al. 1996, A&A, 315, L64
Lemke, D., & Klaas, U. 1999, in The Universe as seen by ISO, ed. P. Cox, & M. F. Kessler, ESA-SP, 427, 55
Ott, S., Gastaud, R., Ali, B., et al. 2001, Astronomical Data Analysis Software and Systems X, ed. F. R. Harnden, Jr., F. A. Primini, & H. E. Payne, ASP. Conf. Ser., 238, 170
O'Sullivan, E., Forbes, D. A., & Ponman, T. J. 1999, MNRAS, 328, 461
Penereiro, J. C., De Carvalho, R. R., Djorgovski, S., & Thompson, D. 1994, A&AS, 108, 461
Popescu, C. C., Tuffs, R. J., Völk, H. J., et al. 2002, ApJ, 567, 221
Ryan-Weber, E., Webster, R., & Bekki, K. 2003, in The IGM/Galaxy Connection: The Distribution of Baryons at $z = 0$, ed. J. L. Rosenberg, & M. E. Putman (Dordrecht: Kluwer), ASSL Conf. Proc., 281, 223
Rupen, M. P., Hibbard, J. E., & Bunker, K. 2001, in Gas and Galaxy Evolution, ed. J. E. Hibbard et al., ASP Conf. Ser., 240, 864
Schneider, S. E. 1985, ApJ, 288, L33
Schweitzer, F., van Gorkom, J. H., & Seitzer, P. 1989, ApJ, 338, 770
Sodroski, T. J., Bennett, C., Boggess, N., et al. 1994, ApJ, 428, 638
Stickel, M., Lemke, D., Klaas, U., et al. 2000, A&A, 359, 865
Stickel, M., Bregman, J. N., Fabian, A. C., White, D. A., & Elmegreen, D. M. 2003, A&A, 397, 503
Stickel, M. 2004, in Recycling Intergalactic and Interstellar Matter, ed. P.-A. Duc et al., Proc. IAU Symp., 217, 108
Stickel, M., van der Hulst, J. M., van Gorkom, J. H., Schiminovich, D., & Carilli, C. L. 2004a, A&A, 415, 95, 2004
Stickel, M., Lemke, D., Klaas, U., Krause, O., & Egner, S. 2004b, A&A, 422, 39
Tonry, J. L., Dressler, A., Blakeslee, J. P., et al. 2001, ApJ, 546, 681
Temi, P., Brighenti, F., Mathews, W. G., & Bregman, J. D. 2004, ApJS, 151, 237
Tuffs, R. J., Popescu, C. C., Pierini, D., et al. 2002, ApJS, 139, 37
Weinberger, R., Temporin, S., & Kerber, F. 1999, ApJ, 522, L17
Williams, B. A., Yun, M. S., & Verdes-Montenegro, L. 2002, AJ, 123, 2417
Xu, C. K., Lu, N., Condon, J. J., et al. 2003 ApJ, 595, 665